Influence of DNA Base Sequence on the Binding Energetics of Actinomycin D†

Susan A. Bailey,‡ David E. Graves,*,‡ Randolph Rill,§ and Glenn Marsch§,‖

Department of Chemistry, University of Mississippi, University, Mississippi 38677, and Department of Chemistry and Institute of Molecular Biophysics, Florida State University, Tallahassee, Florida 32306

Received February 1, 1993; Revised Manuscript Received March 30, 1993

ABSTRACT: The influences of base sequence on the thermodynamic properties associated with the interaction of actinomycin D with DNA are examined. It has been previously established that GpC steps of double-helical DNAs are highly preferred binding sites for actinomycin D. In this study, a series of oligonucleotides was designed and synthesized to probe the effects of flanking base sequence (adjacent to the GpC step) and novel non-GpC binding sites on the binding of actinomycin D. The use of these oligonucleotides provides a direct method for quantitating sequence specificities and actinomycin D binding energetics. Effects of different 5′ and 3′ flanking nucleotides on the interactions of actinomycin with the core GpC binding sites were examined using UV–visible spectrophotometric methods, and changes in binding energetics were quantitated. These studies demonstrate strong actinomycin D binding affinities to both classical GpC and an atypical non-GpC site. Enthalpy and entropy components of the DNA binding energetics for the GpC binding sites are compared and correlated with those determined for actinomycin D binding to the high-affinity non-GpC site of an 11-mer containing TGGGT as the central sequence. This TGGGT site, first suggested to be a high-affinity sequence in our earlier photoaffinity labeling studies, exhibits binding of actinomycin D comparable in strength to that of traditional actinomycin D binding sites (*i.e.*, GpC steps). From these studies, the overall affinity and specific thermodynamic contributions ($\Delta H°$, $\Delta S°$) to binding of actinomycin D are demonstrated to be highly influenced both by the sequence at the intercalation site and by neighboring bases which flank the intercalation site.

The sequence specificity of interactions of actinomycin D with nucleic acids has been the subject of extensive investigation for over 3 decades. A requirement for guanine and preferential binding to GpC steps are thought to be the result of intercalation of the planar phenoxazone ring between the GpC step of the DNA double-stranded helix coupled with the ability of cyclic pentapeptide side chains of the actinomycin D to form hydrogen bond contacts through the carbonyl oxygen of a threonine residue to the guanine 2-amino. This GpC preference was first observed by Muller and Crothers (1968) and Wells *et al.* (1970). A model for the preferential binding of actinomycin D to the GpC step was first proposed by Sobell and Jain (1971) on the basis of X-ray diffraction studies on the 2:1 complex of deoxyguanosine with actinomycin D. Further evidence of the preferred binding to the GpC step has been presented using a variety of biophysical methods: NMR studies of actinomycin D complexed with oligonucleotides containing GpC sequences (Patel, 1974; Krugh & Neely, 1973; Brown, 1984); more recently, DNase I footprinting studies by Lane *et al.* (1983), Fox and Waring (1984), and Goodisman *et al.* (1992); and transcription footprinting studies by Aivasashvilli & Beabealashvilli (1983), Phillips and Crothers (1986), and Phillips *et al.* (1990).

Recently, Kamitori and Takusagawa (1992) determined the structure of actinomycin D complexed with the self-complementary octanucleotide d(GAAGCTTC)$_2$ by X-ray crystallographic methods. Their study revealed that, upon binding actinomycin D, the DNA becomes severely distorted (*i.e.*, kinked) and, interestingly, the cyclic pentapeptide side chains of actinomycin D residing in the minor groove become asymmetrical. Various contacts between the DNA and both the drug chromophore and the side chains were observed, including hydrophobic–hydrophobic interactions between the surface of the minor groove and the proline, sarcosine, and methylvaline residues of the cyclic pentapeptides. Their study predicts that the bases which flank the intercalation site are highly influential in directing actinomycin D binding and

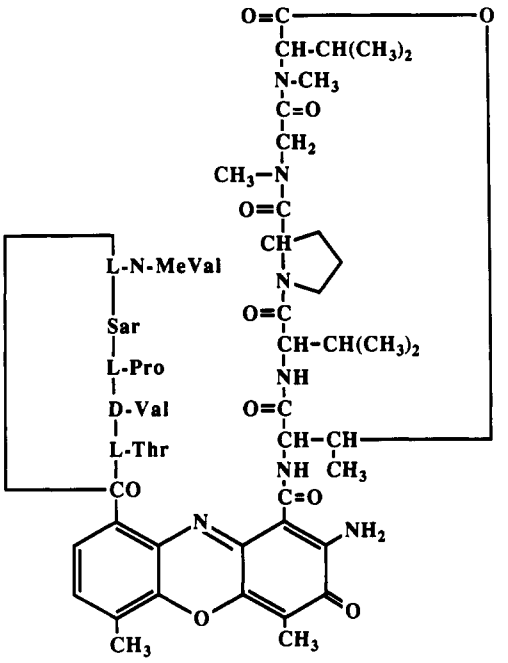

FIGURE 1: Chemical structure of actinomycin D.

† This research was supported in part by grants from the U.S. Public Health Service (Research Grant CA-41474) (D.E.G.), the Elsa U. Pardee Foundation (D.E.G.), and the Department of Energy (Grant ER60588) (R.L.R.).

* Address correspondence to this author at the University of Mississippi. Telephone: (601) 232-7732. FAX: (601) 232-7300.

‡ University of Mississippi.

§ Florida State University.

‖ Present address: Biology & Biotechnology Research Program, Lawerence Livermore National Laboratory, Livermore, CA 94550.

0006-2960/93/0432-5881$04.00/0

suggests that the 5′ flanking base adjacent to the GpC intercalation site is restricted to either A or T, due to hydrophobic and steric interactions.

Recent evidence suggesting strong interactions of actinomycin D with non-GpC DNA sequences has been reported. In 1989, Breslauer and co-workers (Snyder *et al.*, 1989) demonstrated actinomycin D to have a high binding affinity for the $d(CGTCGACG)_2$ duplex. In fact, two molecules of actinomycin D were shown to bind within this duplex, which lacks the typical GC step. In 1989, our laboratories demonstrated a higher order of specificity. Using 7-azidoactinomycin D as a photoaffinity probe and DNA sequencing methods to quantitatively monitor sites of covalent photoaddition, we found that the GpC steps were strongly preferred, but only if the 5′ flanking base was a pyrimidine and the 3′ flanking base was not cytosine (Rill *et al.*, 1989). An unexpected observation from this study was the discovery of a novel, non-GpC actinomycin D binding site indicated by the high reactivity of the second G in the TGGGT sequence. This TGGGT site had not previously been reported as a binding site for actinomycin D and seemingly would require a binding/intercalation model quite different from that proposed for the GpC step.

The influence of neighboring and next-neighboring bases (adjacent to the intercalation site) on actinomycin D binding has become increasingly evident. The footprinting and photoaffinity labeling studies described above confirmed the strong preference of actinomycin D for GpC steps, but revealed a strong dependence of affinity on the bases which flank the intercalation site. In 1988, Chen employed a series of self-complementary decamers of the sequence d(ATAXGCYTAT) to correlate the binding of actinomycin D to different XGCY sites. From these studies, actinomycin D binding was found to decrease in the order of TGCA > CGCG > AGCT ≫ GGCC. The rate of SDS-promoted dissociation of actinomycin from the TGCA decamer was 2 orders of magnitude slower than that from the GGCC decamer. These findings are consistent with our photoaffinity labeling studies, which demonstrated preferential actinomycin D binding to GpC sites flanked on the 5′ side by a pyrimidine and on the 3′ side by a purine.

The following oligonucleotides were examined to determine the effects of base sequence at the intercalation site and at neighboring sites on the binding affinities and energetics of actinomycin D–DNA complex formation. The TCGT duplex

5′-CTATTGCATAC-3′/5′-GTATGCAATAG-3′
(referred to as TGCA)

5′-CTACCGCATAC-3′/5′-GTATGCGGTAG-3′
(referred to as CGCA)

5′-CTATGGGTTAC-3′/5′-GTAACCCATAG-3′
(referred to as TGGGT)

5′-CTATCGTATAC-3′/5′-GTATACGATAG-3′
(referred to as TCGT)

was included in this study as a control and was not expected to be a strong actinomycin D binding site, but with a sequence, composition, and stability similar to those of the other duplexes examined.

EXPERIMENTAL METHODS

Oligonucleotide Preparation. Non-self-complementary deoxyoligonucleotides of specific length and sequence were prepared using an Applied Biosystem DNA synthesizer which uses β-cyanoethyl phosphoramidite chemistry. The crude oligomer was purified on a Pharmacia FPLC system using anion-exchange chromatography (Pharmacia Mono Q). Oligonucleotides were then desalted using a reverse-phase HPLC column containing an acetonitrile gradient (0–30%), which revealed greater than 98% purity of the oligonucleotide. The lyophilized strands were dissolved in 0.01 M sodium phosphate (pH 7.0), 0.001 M disodium ethylenediaminetetraacetate, and 0.1 M sodium chloride. All subsequent experiments were carried out in this buffer. Molar absorptivities for each oligomer were determined by the nearest-neighbor method (Fasman, 1975).

Oligonucleotide Characterization. Stock solutions of single strands were mixed in a 1:1 stoichiometry with their complement to obtain duplexes. Duplex-to-single-strand thermal denaturation profiles for each of the oligonucleotide duplexes were obtained using a Cary 4 (Varian) spectrophotometer equipped with thermostated cell holders, mixers, and a programmable temperature controller (Lauda) which incremented the temperature at 0.25 °C/min. Thermodynamic parameters associated with helix formation were derived from analyses of the change in absorbance at 260 nm (ΔA) versus temperature curves as described by Petersheim and Turner (1983) and Freier *et al.* (1983). Melting curves were fit to a two-state model to obtain $\Delta H°$ and $\Delta S°$ using Enzfitter (Biosoft). Since the melting temperatures of the oligonucleotide duplexes are concentration dependent, all DNA denaturation experiments were performed at identical concentrations, which were also maintained during the drug binding experiments.

Denaturation studies of the oligonucleotides in the presence of bound actinomycin D were also carried out. The amount of actinomycin D to be added was calculated using the following equation:

$$f_b = \frac{K_a[D]}{1 + K_a[D]}$$

where f_b is equal to the fraction of bound DNA (>95%), and [D] is the drug concentration required to obtain 95% bound complex. The duplex oligonucleotide concentrations, binding constants, K_a, and binding densities were previously determined for each of the sequences examined. Thermodynamic parameters for the melting transition in the presence of actinomycin D were obtained in the same manner as described above for the thermal transitions of the DNA duplexes alone.

Actinomycin D–DNA Interaction. Binding of actinomycin D with selected oligonucleotides was monitored by UV–visible spectroscopy. Complex formation with DNA results in a marked change in the visible region of the drug's absorption spectrum and can be utilized as a means to monitor the equilibrium binding of the drug to DNA. Known concentrations of duplex oligonucleotide were pipeted into 10-cm path length cylindrical cells maintained at 10 °C, which were directly monitored by insertion of a thermistor microprobe into the sample cuvettes and displayed on the Cary 4 CRT. As determined from our helix-to-coil transition studies, greater than 95% of the oligomer is in the duplex conformation at this temperature, ionic strength, and DNA concentration. Small aliquots of a known concentration of stock actinomycin D solution were titrated into the sample cell. After each addition, the solution was exhaustively mixed and allowed to reequilibrate to the set temperature. The absorbance was then determined directly at selected wavelengths of maximal absorbance change using the statistical algorithm which signal-averages 300 readings and provides the mean and standard deviation of the absorbance value. Total actinomycin D

concentration (C_t) was maintained at less than 5 μM to circumvent errors associated with the aggregation of actinomycin D in aqueous solution. The absorbance changes of the actinomycin D, resulting from complex formation with the oligonucleotides, were used to quantitate the intrinsic equilibrium binding constant, K_{int}, and the site-exclusion parameter, n. Bound and free drug concentrations (C_b and C_f, respectively) were determined by the equation

$$C_b = \frac{\Delta A}{\Delta \epsilon} \quad \text{and} \quad C_f = C_t - C_b$$

where ΔA is the difference in the absorption between the free and bound drug species and $\Delta\epsilon$ is the difference in the molar absorptivities for the free and bound drug species.

The Scatchard equation was used to determine the binding constant, K, and site-exclusion size, n (drugs bound per duplex), for each of the data sets. The Scatchard equation (Scatchard, 1949) adequately describes the binding of actinomycin D to these duplexes because of the presence of a single binding site, eliminating the need for neighbor exclusion and/or cooperative binding terms. K and n were estimated from an iterative nonlinear least-squares fitting routine (Simplex).

$$\frac{r}{C_f} = K(1 - nr)$$

The change in absorbance of the drug as a function of complex formation with DNA allows experimental determination of ϵ_b (molar absorptivity of the fully bound drug species). In the case of actinomycin D–calf thymus DNA, this value was determined to be 12 000 M^{-1} cm^{-1} (Muller & Crothers, 1968), representing the average value for a composite of all potential binding sites on the native DNA. However, in the case of these selected oligonucleotide duplexes, a primary concern was that, with only one potential binding site within the duplex, the molar absorptivity of the bound drug species may differ for each duplex due to the varying influences of the physical and chemical environment, which result from differences in the base sequence. For the Scatchard analysis described above, molar absorptivities for the bound drug species were determined (on a limited basis due to the small quantities of oligonucleotides). For each of the oligonucleotide duplexes, the ϵ_b values were found to be comparable to the ϵ_b values obtained for native calf thymus DNA, within 10%.

In an effort to verify the accuracy of these binding isotherms, an alternative method was employed which examined complex formation on the basis of a simple site interaction model from Langmuir binding isotherms, as reported by Wadkins and Jovin (1991). Determination of the duplex concentrations that produce changes in the absorbance which are equal to one-half of the extrapolated maximum change in absorbance values provides a qualitative measure of the relative binding constant. With this method, binding isotherms were obtained at 10 °C using a reverse-titration method where aliquots of a known concentration of oligonucleotide duplex were titrated into a fixed concentration (and volume) of actinomycin D. The absorbance at 440 nm was monitored as aliquots of DNA were added. The change in absorbance (correcting for dilution effects) was recorded and plotted against the oligonucleotide (duplex) concentration, and the resulting binding isotherms were analyzed by nonlinear least-squares fitting routine. Values for K and n were shown to be in excellent agreement with those obtained by Scatchard analysis.

Thermodynamic Analysis of Binding Data. The fixed ratio method outlined by Chaires (1985) and Shimer *et al.* (1988) was used to provide data for van't Hoff analyses because the amounts of oligonucleotides required were limited. Data were obtained by adding a known concentration of drug to the DNA solution at 10 °C and determining the concentration of free and bound drug using eqs 1 and 2 as described above. The temperature was then increased to 30 °C and the mixture was allowed to equilibrate for 6 h. After thermal equilibrium had been achieved, the absorbance was determined and the temperature was decreased in 5-deg increments. The sample was allowed to equilibrate for 3 h at each new temperature, and the amounts of free and bound drug were redetermined by monitoring the change in absorbance. Due to the limited thermal stability of the oligonucleotide duplexes, the accessible temperature range for van't Hoff analyses was restricted to between 0 and 30 °C. At temperatures greater than 30 °C, helix-to-coil transitions of the oligonucleotide were observed, leading to energetics dominated by helix denaturation, rather than actinomycin D binding. The Scatchard equation was used to calculate K_a from the measured r and r/C_f values at each temperature. A linear least-squares analysis of a plot of the ln (K_a) versus $1/T$ (K) was used to estimate the apparent enthalpy of binding from the van't Hoff relationship:

$$\frac{d \ln K_a}{d(1/T)} = -\frac{\Delta H°}{R}$$

where R is the gas constant.

This van't Hoff analysis of ligand binding to DNA has been shown to provide results identical to those obtained by calorimetric methods (Sauer *et al.*, 1984) which require prohibitively high concentrations of oligonucleotides. Determination of the enthalpy of binding by this method provides sufficient data for a full thermodynamic profile to be estimated by the following relationships:

$$\Delta G° = -RT \ln K$$

$$\Delta S° = \frac{-(\Delta G° - \Delta H°)}{T}$$

RESULTS

DNA Stability as a Function of Sequence. Enthalpy and entropy components associated with duplex formation of selected oligonucleotides both in the absence and presence of actinomycin D are provided in Table I. The error associated with these data is estimated to be ±10% due to the lower T_m values associated with the lengths and concentrations of oligonucleotides used in these experiments. The thermodynamic stabilities of these oligomers are reflected by the $\Delta H°$ and $\Delta S°$ values and are shown to be highly sequence dependent. Thermal stability (*i.e.*, T_m) generally correlates with the relative GC content of each duplex. The CGCA duplex, with 55% GC content exhibits, the highest T_m at 44 °C, the TGGGT duplex (45% GC) has a T_m of 38 °C, and the duplexes TGCA and TCGT, both having 36% GC content, exhibit the lowest T_m values at 37 and 31 °C, respectively. Subtle changes in the internal base pairs of these duplexes result in marked differences in the thermodynamic properties associated with duplex formation; for example, the reversal in sequence from GCA to CGT results in a substantial decrease (6 °C) in the T_m values of the two oligonucleotides.

All of the duplexes examined exhibit helix destabilization enthalpy and entropy values of approximately 55–75 kcal/mol and 150–200 eu, respectively. The similarities in melting parameters reflect the similarities in the oligonucleotides themselves (*i.e.*, identical lengths and comparable sequences). Values for the predicted melting enthalpy were calculated using the nearest-neighbor stacking interactions of Breslauer

Table I: Thermodynamic Profile Associated with Duplex Formation[a]

sequence[b]	% GC	free duplex T_m (°C)	duplex + drug ΔT_m (°C)	observed $-\Delta H°$ (kcal/mol)	predicted $-\Delta H°$ [c] (kcal/mol)	$\Delta S°$ (cal/mol·K)
5′-CTACCGCATAC-3′ GATGGCGTATG	55	44	9	70	80	196
5′-CTATGGGTAC-3′ GATACCCAATG	45	38	7	74	78	213
5′-CTATTGCATAC-3′ GATAACGTATG	36	37	9	53	76	148
5′-CTATCGTATAC-3′ GATAGCATATG	36	31	1	55	73	158

[a] T_m, $\Delta H°$, and $\Delta S°$ were determined by a nonlinear least-squares algorithm in ENZFITTER (Biosoft). [b] Oligonucleotide concentrations are as follows: CGCA, 1.6 μM; TGCA, 1.7 μM; TGGGT, 1.7 μM; TCGT, 1.7 μM (duplex). All melting profiles determined in 0.01 M sodium phosphate buffer (pH 7.0), 0.001 M disodium ethylenediaminetetraacetate, 0.1 M sodium chloride. [c] Predicted $\Delta H°$ values for the duplex denaturation were determined by the nearest-neighbor analysis of Breslauer and co-workers (Breslauer et al., 1986).

and co-workers (Breslauer *et al.*, 1986). These predicted values were in good agreement with those obtained from our denaturation experiments (Table I).

The oligonucleotide melts carried out in the presence of 1:1 actinomycin D were performed to determine the extent, if any, of helix stabilization resulting from drug binding. Actinomycin D had previously been shown to be a DNA helix stabilizer (McGhee, 1976; Chen, 1988b). In the case of these selected oligonucleotides helix stabilization was also observed, the degree of which was dependent upon base sequence and actinomycin D binding affinity. The sequences showing the greatest ΔT_m values (+9 °C) are the TGCA and CGCA sequences, both of which contain the classical GpC step for actinomycin D binding and show the highest binding constants of the sequences examined. The degree of helix stabilization (ΔT_m) correlates with the magnitude of the binding constant. ΔT_m for TGGGT is +7 °C, while the ΔT_m for TCGT is +1 °C (Tables I and II). Actinomycin D binding to TGGGT, the non-GpC site, also confers helix stabilization, perhaps implying similarity in binding with the other GpC sites.

Interactions of Actinomycin D with Selected Oligonucleotides. The interactions of actinomycin D with selected oligonucleotides were examined by monitoring the change in the visible spectrum of the drug upon the addition of DNA of selected length and sequence. The interaction of actinomycin D with native (calf thymus) DNA has been well characterized by visible spectroscopy (Muller & Crothers, 1968; Chiao *et al.*, 1979). Intercalative binding of actinomycin D is shown to result in a significant decrease in the absorbance and a red shift of 10 nm. The spectrophotometric titration curves generated upon titration of actinomycin D with an oligonucleotide containing the classic TGCA binding site are compared with curves resulting from the interaction of actinomycin D with the nonclassical TGGGT sequence. As shown in Figure 2, the titration curves were nearly identical, with both oligomers producing hypochromic and bathochromic effects indicative of similarities in binding environments for the phenoxazone ring. Spectra obtained upon complex formation by both duplexes exhibited isosbestic points at 458 nm and shifts in λ_{max} of ~10 nm, similar to the spectral properties observed from native DNA binding to actinomycin D (Muller & Crothers, 1968).

Scatchard plots describing actinomycin D binding to the higher affinity oligonucleotides are shown in Figure 3. Solid lines drawn through the data represent best fits using the linear Scatchard equation. Parameters used to fit this equation to the experimental data are provided in Table II. These data reveal that oligomers which contain central GC steps, TGCA and CGCA, bind actinomycin D with the highest binding

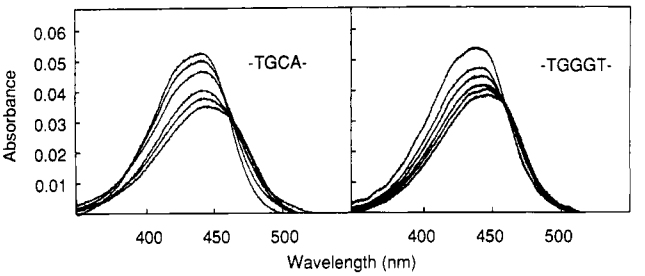

FIGURE 2: Representative absorption spectra comparing the interaction of actinomycin D with the 5′-CTATTGCAAT-3′/5′-GATAACGTATG-3′ duplex (left panel) and 5′-CTATGGGTTAC-3′/5′-GATACCCAATG-3′ (right panel). In both cases, the free actinomycin D exhibits the maximal absorption spectrum. As oligonucleotide (duplex) is added, the spectrum is observed to undergo a 15-nm shift from 440 to 465 nm, accompanied by a decrease in absorbance of the actinomycin D chromophore. An isosbestic point is observed in the case of both duplexes at 460 nm. Spectra were obtained on a Cary 4 UV–visible spectrophotometer by titrating small volumes of concentrated oligonucleotide duplex (3 mM) into dilute actinomycin D (<2.5 μM). All solutions were maintained at 10 °C prior to and during spectral acquisition. Both the drug and DNA were dissolved in 0.01 M sodium phosphate buffer, pH 7.0, 0.001 M disodium ethylenediaminetetraacetate, and 0.1 M sodium chloride.

affinities: 4.0×10^6 M^{-1} (duplex) and 2.5×10^6 M^{-1} (duplex), respectively. As suggested by Kamitori and Takusagawa (1992), the TGCA duplex exhibits a binding constant larger than that of the CGCA duplex, but the difference is modest. The oligonucleotide containing the TGGGT sequence exhibits a slightly lower binding constant of 1.5×10^6 M^{-1} (duplex). For all of the high-affinity oligonucleotide duplexes, the binding site size was found to be approximately 1 (±0.2), indicating that each duplex contains a single actinomycin D binding site. In contrast, the control sequence TCGT has a very low binding constant, $<5 \times 10^3$ M^{-1} (duplex), and a site-exclusion size of 0.3, corresponding to approximately three nonspecific binding sites on this oligomer duplex (data not shown). Thus, this duplex, which contains terminal sequences identical to those of the high-affinity duplexes, lacks a single high-affinity site.

Analyses of binding isotherms as described above rely on the accurate determination of ϵ_b (molar absorptivity of the fully bound species of actinomycin D). With the limited stocks of oligonucleotides available, we were able to experimentally estimate ϵ_b for each of the sequences examined. The values were nearly equivalent for TGCA-, CGCA-, and TGGGT-containing oligonucleotides and within ±10% of that determined for native calf thymus DNA (Muller & Crothers, 1968). In addition, we employed an alternate method for determining the binding constants based on the simple site interaction model described by Wadkins and Jovin (1991), which does not rely on the quantitative determination of ϵ_b. By design, these oligonucleotides were expected to contain only a single

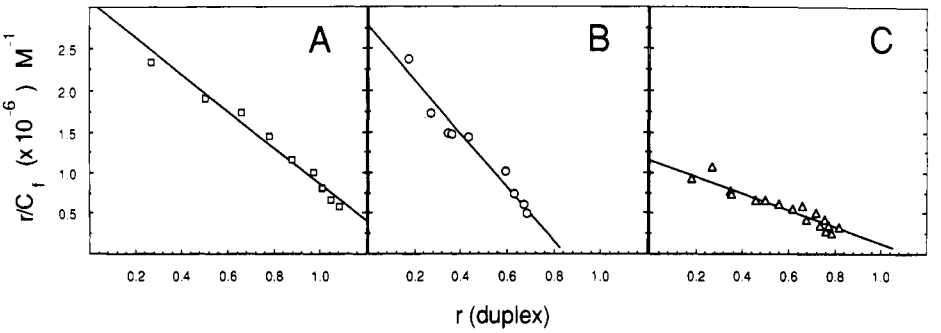

FIGURE 3: Scatchard plots comparing the interactions of actinomycin D with TGCA (A), CGCA (B), and TGGGT (C). Binding isotherms were obtained by serial titration of actinomycin D into a known concentration of oligonucleotide and monitoring the absorbance change at 440 nm using a Cary 4 UV–visible spectrophotometer. Temperature was maintained throughout the experiment at 10 °C. All solutions were dissolved in 0.01 M sodium phosphate buffer, pH 7.0, 0.001 M disodium ethylenediaminetetraacetate, and 0.1 M sodium chloride. Drug concentrations were maintained at concentrations below 5 μM to minimize aggregation effects.

Table II: Thermodynamic Data for the Interactions of Actinomycin D with Selected Oligonucleotides

sequence	K_{int} (M^{-1})[a]	K_{int} (M^{-1})[b]	n (duplex)[a]	$\Delta G°$ (kcal/mol)[c]	$\Delta H°$ (kcal/mol)[d]	$\Delta S°$ (cal/mol·K)[e]
5′-CTACCGCATAT-3′ GATGGCGTATA	2.5×10^6	2.4×10^6	1.2	−8.3	−6.1	+8
5′-CTATTGCATAT-3′ GATAACGTATG	4.0×10^6	4.6×10^6	0.8	−8.5	−2.5	+21
5′-CTATGGGTAC-3′ GATACCCAATG	1.5×10^6	1.4×10^6	1.0	−8.0	−3.7	+15
5′-CTATCGTATAC-3′ GATAGCATATG	negligible binding observed					

[a] Binding parameters derived from Scatchard analysis. [b] Binding constants derived from nonlinear least-squares fit of reverse titration binding isotherms (Kaleida-Graph). [c] Calculated from K_{int} from the relation $\Delta G° = -RT \ln K$. [d] Values obtained from the slope of the van't Hoff plots. [e] Entropy estimated from the relation $\Delta S° = -(\Delta G° - \Delta H°)/T$.

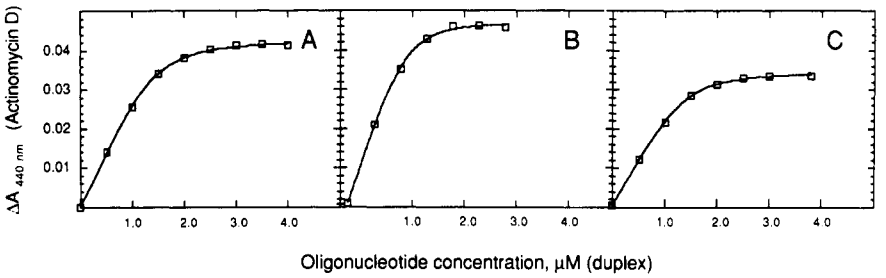

FIGURE 4: Binding isotherms of actinomycin D interacting with TGCA, CGCA, and TGGGT. Data were obtained by the reverse titration method, where a dilute solution of actinomycin D (<1 μM) is titrated with a concentrated stock solution (3 mM (duplex)) of oligonucleotide. Temperature was maintained at 10 °C. The solid line represents the best nonlinear least-squares fit to the data. Curves were fit for the number of binding sites (n) and K_a using the interative nonlinear least-squares method until the difference in successive iterations was less than 0.01%. Analyses of these binding curves provide K_a values of 4.25, 4.0, and 1.5 ($\times 10^6$ M^{-1}), with n values of 1 ± 0.2, respectively.

actinomycin D binding site; thus, no cooperativity term was required and a binding site size of 1 was assumed. Changes in the absorbance of actinomycin D at 440 nm were plotted as a function of the volume of oligonucleotide (duplex) added and were used to generate the binding isotherms shown in Figure 4. Figure 4A–C shows the titrations of actinomycin D with TGCA, CGCA, and TGGGT, respectively. Solid lines are fits to the data as described in the Experimental Methods section. As shown in Table II, DNA binding parameters estimated in this manner were consistent with those obtained through Scatchard analyses.

Thermodynamic Properties. van't Hoff enthalpies and entropies for actinomycin D–oligonucleotide interactions were estimated using the fixed ratio experiments described by Chaires (1985) and Shimer *et al.* (1988) (Figure 5). The $\Delta G°$ values obtained for the interaction of actinomycin D with TGCA, CGCA, and TGGGT were quite similar, ranging from −8.0 to −8.5 kcal/mol. In contrast, enthalpy and entropy contributions varied dramatically as a function of the base sequence of the DNA duplexes.

The interaction of actinomycin D with TGCA is characterized by a binding enthalpy of −2.5 kcal/mol and an entropy of +21 eu. The interaction of actinomycin with the TGGGT duplex exhibits an even more favorable binding enthalpy ($\Delta H°$ = −3.7 kcal/mol), almost 50% more favorable than that of the classic TGCA oligomer. Enthalpies of actinomycin D binding to both the TGCA and TGGGT oligomers were similar to the values for the interactions of actinomycin D with calf thymus DNA reported by Gellert *et al.* (1965) and similar to those for oligonucleotides reported by Snyder *et al.* (1989). These negative enthalpy values are modest in comparison with other intercalators such as ethidium and daunomycin, which are characterized by DNA binding enthalpies ranging from −8 to −12 kcal/mol (Marky *et al.*, 1983; Britt, 1986). The small negative enthalpies of binding of actinomycin D to these oligonucleotide duplexes suggest that a relatively small gain in binding energy is complemented by a large positive entropic driving force resulting from solvent displacement upon formation of the drug–DNA complex. The more favorable binding enthalpy of TGGGT may result from improved

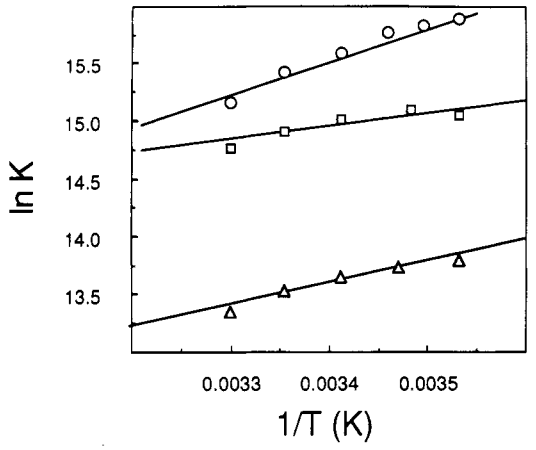

FIGURE 5: van't Hoff plots for the interaction of actinomycin D with oligonucleotides containing the central sequences of TGCA (□), CGCA (○), and TGGGT (△). Solid lines represent linear least-squares fits to the data. Equilibrium constants (K_a) were obtained both by complete titrations as well as by raising the temperature of the sample containing a fixed ratio of drug and DNA, as described in the Experimental Methods section.

stacking interactions or from the formation of an additional contact between the drug chromophore and/or pentapeptide chains in comparison with the case of TGCA.

Surprisingly, complexation of actinomycin D with CGCA is characterized by a larger, more negative enthalpy ($\Delta H°$ = –6.1 kcal/mol), nearly twice the value observed for the other sequences examined. This increased negative enthalpy is compensated by a decreased entropy relative to the other oligonucleotide duplexes, resulting in similar binding free energies. The observed variations in the binding enthalpies and entropies demonstrate strong, though perhaps subtle, influences of sequence on the mechanism(s) through which actinomycin D interacts with DNA.

DISCUSSION AND CONCLUSION

Bases flanking the intercalation site are shown to play a major role in influencing both the binding affinities and the thermodynamic mechanism(s) associated with actinomycin D–DNA interactions. Earlier photoaffinity labeling studies from our laboratories revealed a novel actinomycin D binding site consisting of the sequence TGGGT, with the chromophore located nearest the central G. Examination of the binding properties of actinomycin D binding to a GpG step is of considerable interest since it would, by definition, require a distinctly different binding mechanism (and geometry) from that proposed in the Sobell model (Sobell *et al.*, 1971; Jain & Sobell (1972)). Their model describing the geometry of the actinomycin D–DNA complex requires the presence of the 3′-C:G pair for effective binding to occur and for hydrogen bond contacts between the cyclic pentapeptide rings located in the minor groove and the 2-amino protons of the adjacent 5′-guanines on opposite strands, related by 2-fold symmetry to the chromophore intercalation site. In an effort to correlate the classical GpC sites with the nonclassical TGGGT site, we designed and prepared several non-self-complementary oligomers whose internal sequences consisted of either classical GpC sites, TGGGT site, or a nonbinding site such as a CpG step. The flanking sequences were expected to exhibit low affinity for actinomycin D as was observed.

Actinomycin D binds the TGCA sequence with the highest affinity ($K = 4 \times 10^6$ M^{-1}), as would be expected from the studies of Kamitori and Takusagawa (1992). They predicted a GpC step flanked by either an A or a T on the 5′ side to be the best binding site for actinomycin D. This site is also in agreement with footprinting data and Chen's findings, which demonstrated TGCA to be the highest affinity and slowest dissociating site in his comparison of XGCY-containing dodecamers containing XGCY sites (Chen, 1988a). Interestingly, our data reveal a relatively strong binding site to be CGCA (2.5×10^6 M^{-1}), which would not have been predicted by Kamitori and Takusagawa but is consistent with the footprinting results (Goodisman & Dabrowiak, 1992). The binding of actinomycin D to the TGGGT duplex is comparable to the binding observed for the GpC-containing duplexes mentioned above. As predicted, actinomycin D binds poorly to the TCGT-containing duplex (control sequence), demonstrating its inability to substitute a CpG or a GpT step for a GpC step.

The oligonucleotides used in this study reveal that changes in both the sequence of the intercalation site and the sequence of bases which flank the intercalation site markedly influence the magnitude of the actinomycin D binding enthalpies. Earlier studies by Breslauer and co-workers using microcalorimetric methods, which determined the $\Delta H°$ of actinomycin D binding to oligonucleotides of selected length and sequence, revealed relatively low binding enthalpies (–2 to –2.5 kcal/mol) (Marky *et al.*, 1983; Snyder *et al.*, 1989). The enthalpy of the interaction of actinomycin D with TGCA that we determined ($\Delta H°$ = –2.5 kcal/mol) is identical to the value reported by Snyder *et al.* (1989). Binding of actinomycin D to TGGGT is characterized by a slightly more favorable binding enthalpy, –3.7 kcal/mol. Thus, the slightly lower affinity ($\Delta G°$) of binding at this site cannot be readily attributed to the loss of the typical H-bonding pattern observed for binding in the GpC step. The most dramatic difference in binding enthalpies is observed in the comparison of enthalpy values of TGCA with CGCA, with the latter sequence exhibiting the most favorable binding enthalpy ($\Delta H°$ = –6.1 kcal/mol) at more than twice that typical of other high-affinity sites and close to that of ethidium and other simple intercalators. Surprisingly, this binding enthalpy does not follow the pattern observed for either TGCA or TGGGT and could imply a different binding mechanism and/or geometry.

The interactions of actinomycin D with TGCA and TGGGT are accompanied by relatively small negative enthalpies and large increases in entropy. This small $\Delta H°$ is indicative of a small net change in the overall binding energies as the drug molecule replaces the water in the minor groove of the DNA and the area surrounding the actinomycin D, while the large positive $\Delta S°$ may result from the displaced water being transferred to the bulk water/solvent. In addition, the large negative $\Delta H°$ value observed for the CGCA duplex suggests that binding of actinomycin D to this sequence may involve stabilizing stacking interactions between the phenoxazone ring and the base pairs making up the intercalation site and/or additional contacts with the cyclic pentapeptide side chains, depending on the flanking sequences to the intercalation site.

Our examination of the previously unreported actinomycin D binding site, TGGGT, demonstrates that this sequence binds actinomycin D with an affinity comparable to those of the sequences containing GpC steps previously established as highly preferred binding sites, thus confirming that the photoaffinity labeling experiments described previously are reflective of noncovalent binding at this site. The biological implications of actinomycin D binding to the TGGGT site are quite interesting. The TGGGT sequence and similar sequences are frequently found in several oncogenes and promoters. For

example, the *c-myc* oncogene contains several repeats of $T(G)_nT$ and is the target of current drug therapy research in which the ability of guanine-rich areas to form triplex structures is utilized (Durland *et al.*, 1990).

The differences in binding thermodynamics (*i.e.*, $\Delta G°$ and $\Delta H°$) for the two sequences, CGCA and TGCA, can be attributed to flanking base effects, since it is only the two bases that immediately flank the GC step that differ between the two duplexes. A comparison of these oligonucleotides allows for detecting sequence selectivity and provides a means to begin to unravel the exact mechanisms of actinomycin D binding to DNA. Although thermodynamics cannot provide direct structural insight into this sequence selectivity, the fact that these sequence changes result in marked differences in binding enthalpies may suggest that the binding mechanisms are highly sequence dependent.

REFERENCES

Aivasashvilli, V. A., & Beabealashvilli, R. S. (1983) *FEBS Lett. 160*, 124–128.

Breslauer, K. J., Frank, R., Blocker, H., & Marky, L. A. (1986) *Proc. Natl. Acad. Sci. U.S.A. 83*, 3746–3750.

Britt, M., Zunio, F., & Chaires, J. B. (1986) *Mol. Pharmacol. 29*, 74–80.

Brown, S. C., Mullis, K., Levenson, C., & Shafer, R. H. (1984) *Biochemistry 23*, 403–408.

Chaires, J. B. (1985) *Biopolymers 24*, 403–415.

Chen, F.-M., (1988a) *Biochemistry 27*, 1843–1848.

Chen, F.-M., (1988b) *Biochemistry 27*, 6393–6397.

Chiao, Y. C. C., Rao, K. G., Hook, J. W., III, Krugh, T. R., & Sengupta, S. K. (1979) *Biopolymers 18*, 1749–1792.

Durland, R. H., Kessler, D. J., Duvic, M., & Hogan, M. (1990) in *Molecular Basis of Specificity in Nucleic Acid-Drug Interactions* (Pullman, B., & Jortner, J., Eds.) pp 565–578, Kluwer Academic Publishers, Dordrecht, The Netherlands.

Fasman, G. D., Ed. (1975) *CRC Handbook of Biochemistry and Molecular Biology*, 3rd ed., Vol. I, p 589, Chemical Rubber Publishing Co., Cleveland, OH.

Fox, K. R., & Waring, M. J. (1984) *Nucleic Acids Res. 12*, 9271–9285.

Freier, S. M., Petersheim, M., Hickey, D. R., & Turner, D. H. (1983) *Biopolymers 22*, 1107–1131.

Gellert, M., Smithy, C. E., Neville, D., & Felsenfeld, G. (1965) *J. Mol. Biol. 11*, 445–457.

Goodisman, J., & Dabrowiak, J. C. (1992) in *Advances in DNA Sequence Specific Agents* (Hurley, L., Ed.) Vol. 1, pp 25–49, JAI Press, Greenwich, CT.

Goodisman, J., Rehfuss, R., Ward, B., & Dabrowiak, J. C. (1992) *Biochemistry 31*, 1046–1058.

Jain, S. C., & Sobell, H. M. (1972) *J. Mol. Biol. 68*, 1–20.

Kamitori, S., & Takusagawa, F. (1992) *J. Mol. Biol. 225*, 445–456.

Krugh, T. R., & Neely, J. W. (1973) *Biochemistry 12*, 1775–1782.

Lane, M. J., Dabrowiak, J. C., & Vournakis, J. N. (1983) *Proc. Natl. Acad. Sci. U.S.A. 80*, 3260–3264 (1983).

Marky, L. A., Snyder, J. G., Remeta, D. P., & Breslauer, K. J. (1983) *J. Biomol. Struct. Dynam. 1*, 487–507.

McGhee, J. D. (1976) *Biopolymers 15*, 1345–1375.

Muller, W., & Crothers, D. M. (1968) *J. Mol. Biol. 35*, 251–290.

Patel, D. J. (1974) *Biochemistry 13*, 2396–2402.

Petersheim, M., & Turner, D. H. (1983) *Biochemistry 22*, 256–263.

Phillips, D. R., & Crothers, D. M. (1986) *Biochemistry 25*, 7355–7362.

Phillips, D. R., Cullinane, C., Trist, H., & White, R. J. (1990) *Anti-Cancer Drug Des. 5*, 21–29.

Rill, R. L., Marsch, G. A., & Graves, D. E. (1989) *J. Biomol. Struct. Dynam. 7*, 591–605.

Sauer, B. B., Flint, R. A., Justice, J. B., & Trowbridge, C. G. (1984) *Arch. Biochem. Biophys. 234*, 580–584.

Scatchard, G. (1949) *Ann. N. Y. Acad. Sci. 51*, 660–672.

Shimer, G. H., Jr., Wolfe, A. R., & Meehan, T. (1988) *Biochemistry 27*, 7960–7966.

Snyder, J. G., Hartman, N. G., D'Estantoit, B. L., Kennard, O., Remeta, D. P., & Breslauer, K. J. (1989) *Proc. Natl. Acad. Sci. U.S.A. 86*, 3968–3972.

Sobell, H. M., & Jain, S. C. (1972) *J. Mol. Biol. 68*, 21–34.

Sobell, H. M., Jain, S. C., Sakore, T. D., & Nordman, C. E. (1971) *Nature New Biol. 231*, 200–205.

Wadkins, R. M., & Jovin, T. M. (1991) *Biochemistry 30*, 9469–9478.

Wells, R. D., Larson, J. E., Grant, R. C., Shortle, B. E., & Cantor, C. E. (1970) *J. Mol. Biol. 54*, 465–497.